

Analytical Solutions for Long-Wide-Channel Thick-Base MOS Transistors

I. Effects of Remote Boundary Conditions and Body Contacts

Bin B Jie¹⁾ and Chih-Tang Sah²⁾

¹⁾ bb_jie@msn.com, IME, Peking University, China

²⁾ tom_sah@msn.com, University of Florida, USA

Abstract

Analytical solutions and computed characteristics for long-wide-channel thick-base MOS transistors are reported. The second generation industrial-consensus surface potential approach is used. Decomposition of the 2-Dimensional transistor problem into two 1-D problems follows the 1966-Pao-Sah current- or Y-equation and the 1965-Sah-Pao voltage- or X-equation as modified by 2002-Gildenblatt-McAndrew-Victory and 2004-Sah-Jie to correct the physical-unreality imaginary electric field at flatband. The effects of the remote body boundary condition and contact type on drain-current vs gate-voltage characteristics are described, including the two asymptotic contact types (short-circuit and open-circuit) and geometry, as well as the two ancient approximations to avoid the divergent bipolar-transistor-like minority-carrier currents at MOS flatband.

Keywords: MOS transistor, double integral drain current y-equation, surface-potential gate-voltage x-equation, flatband current, remote contact types and lengths

1. Introduction

Design of MOS integrated circuits containing many transistors requires compact (simple and fast but still accurate) transistor models for use in the circuit simulator. The first generation industrial standard MOS transistor compact models for the past decades have been the 1964-Sah **threshold-voltage model** [1] and its extensions to include body dopant impurities as bulk-charges introduced in 1965-Sah-Pao [2], and the diffusion current, mobility variations, and short channel effects reviewed by the 1993-2007 Arora textbook [3]. Advanced second generation compact models have been under recent development for new technologies for smaller and new transistor structures, such as the FIN structure [4], and for analog circuits. These advanced compact models are following two approaches [5]: the **inversion-charge-based** compact modeling reviewed in the 2007 textbook of Galup-Montoro and Schneider [6] and the **surface-potential-based** compact modeling. A surface-potential-based compact modeling approach (the PSP authored by Gennady Gildenblatt) was selected recently (Fall-2006) by the 30 international corporate members of the international Compact Modeling Council to develop the second generation industrial standard MOS transistor compact models.

MOS transistor modeling, using the surface potential as the independent variable to compute terminal currents and voltages, originated from the two old reports on the MOS transistor theory [1]: the 1965-Sah-Pao [2] and 1966-Pao-Sah [7]. In this 40+year-old Sah-Pao theory, the two-dimensional long-wide-channel and thick-base (LWC-TkB) transistor problem is decomposed into the two coupled one-dimensional problems: the x-direction surface-potential vs gate-voltage relationship described in the 1965-Sah-Pao paper [2], and the one-dimensional double integration of the y-direction gradient of the electron quasi-Fermi potential described by 1966-Pao-Sah [7]. Two corrections were made on these two one-dimensional problems.

(1) The self-consistent x-equation or voltage-equation was derived rigorously and numerically tested in 2004-Sah-Jie [1] which includes two corrections: the remote boundary condition dc steady-state space-charge-neutrality and the minority carriers which is important at flatband. These two corrections removed the erroneous imaginary x-component of the dc electric field at flatband, which was discovered by 2002-Gildenblatt-McAndrew-Victory [8] and overcome via mathematical conditioning the 1965-Sah-Pao x-equation.

(2) The one-dimension 4-component drain current equation was derived from the 1996-Sah [9] two-dimension space-charge theory of MOS transistors and numerically implemented by Jie and Sah [10], to replace and test the accuracy and error of the 1978-Brews charge-sheet model [11] which was derived semi-empirically from the 1966-Pao-Sah double integral [7].

This paper reports our investigation of the effects of the remote boundary conditions, described in (1) above on the current-voltage characteristics of the inversion long-wide channel and thick-base MOS transistor. Spatially constant dopant impurity concentration is assumed. Report on spatial variation is delayed due to its substantially more stringent demand on numerical precision, requiring 64-bit floating-point processor not yet available in the PC Windows operating system software and hardware. Section 2 summarizes the surface-potential-based gate-voltage- or x-equation and double-integral drain-current- or y-equation. Our model-number convention using digits to specify the models and their approximations and assumptions are given in Table 1. Section 3 illustrates the effects of remote contact types and lengths, and the absence or presence of the flatband current on the drain-current versus gate voltage characteristics. Section 4 shows the preliminary results of the effects of y-dependent dopant impurity concentration.

2. MOS transistor theory

2.1 Surface-potential gate-voltage equation

The surface-potential gate-voltage equation was first derived for the two-terminal MOS capacitance [1]. It was extended to MOS transistors in 1965-Sah-Pao [2] which made five assumptions. (1) The electric potential at the remote boundary is independent of y -direction, and set as the reference, $U(x=\infty, y) = U_\infty(y) = 0$. (2) The x -component of the electric field at the remote boundary is zero, $\partial U(x=\infty, y) / \partial x = 0$. (3) The quasi-Fermi potential of the majority carriers is x -independent and equal to the equilibrium value. (4) The quasi-Fermi potential of the minority carriers is independent of x in the surface space-charge region which then decreases to its equilibrium value at the remote boundary $x=\infty$. (5) Both electron and hole quasi-Fermi potentials are assumed x -independent when integrating x -component of the Poisson equation, twice, from the surface or interface, $x=0$, to the remote boundary, $x=\infty$, to give the x -equation or the voltage-equation [1]. This x -equation had been used for 40+ years until the imaginary electric field in a small range of surface potential near flatband was found in 2002 [8]. As discussed in [12], the physical basis for this 1965-Sah-Pao x -equation is a long-wide-channel and thick-base MOS transistor with the remote Si-Body/metal boundary of an ohmic contact or infinite interfacial recombination velocity, i.e. a short-circuit. {Realistic metal/semiconductor contact is not a zero-resistance perfect ohmic contact. See Sections 560-564, especially 562 and Eq.(564.10) on p. 496 of [13]. }

To solve the imaginary electric field issue, a self-consistent x -equation was rigorously derived [1]. This 2004-Sah x -equation removes the two inconsistent 1965-Sah-Pao assumptions, by assuming that both electron and hole quasi-Fermi potentials are x -independent from the interface $x=0$ to the remote boundary $x=\infty$ and by including the nonequilibrium minority-carrier concentration in the remote space-charge neutrality condition.

There are other types of remote contact, such as a p^{++}/p^- hi/lo junction in a practical thick-body inversion nMOS transistor, an n/p junction in a practical pMOS transistor with a ion-implanted n -basewell on a p -body silicon wafer, a tunnel diode {see the section 570 of [13]}, an ohmic contact {see sections 580-583 of [13]}. To illustrate the effects of the remote contact on the drain-current vs gate-voltage characteristics, we shall use the two remote boundaries: (1) the short-circuit assumed by the 1965-Sah-Pao x -equation [2] and (2) the open-circuit used in the 2004-Sah x -equation [1].

2.2 Double-integral drain-current equation

The double integral drain current was first derived and computed numerically in 1966-Pao-Sah [7] which integrated the y -gradient of quasi-Fermi potential of electrons $\int N(x, y) \times [\partial V_N(x, y) / \partial y] dx$ to give the drain or channel current. The original 1966-Pao-Sah drain current equation

made the following assumptions. (1) There is no hole current in the drain current. (2) Electrons flow only along the y -direction. (3) Electron current beyond the intrinsic potential point, $x=X_{\text{INTRINSIC}}$, at $U(x=X_{\text{INTR}}, y) = U_F$, to $x=\infty$, is neglected to avoid divergence at Flatband ($U_S=0$) and to avoid the numerical integration divergence as $x \rightarrow \infty$.

When we evaluated the one-dimensional 9604 four-component drain current equation in [10], the double-integral drain current equation was modified to avoid flatband divergence by subtracting the divergent flatband current from the infinitely thick body or basewell layer of the p -type region, using $[N(x, y) - N(\infty, y)] \times [\partial V_N(x, y) / \partial y]$.

In this paper, the deviation or error from subtracting the flatband current in these two ways: ($x=0$ to $x=X_i$) and $N(x, y) - N(\infty, y)$, are computed for the two electrical asymptotic remote boundary conditions, open-circuit and short-circuit, and also their mixture.

Table 1 Seven models labeled by JJVVFXY

Model	Model description
66650109	Shorten as 66650I. LWC-TkB transistor with the full-length short-circuit remote body contact. Including Flatband current. The thickness of drain current is from $x=0$ to the intrinsic point $U(x, y) = U_F$.
66650109	Shorten as 66650I. LWC-TkB transistor with the full-length short-circuit remote body contact. Including Flatband current. The thickness of drain current is from $x=0$ to the point at $U=10^{-6}U_F$.
66651109	Shorten as 66651I. LWC-TkB transistor with the full-length short-circuit remote body contact. Subtracting flatband current. The thickness of drain current is from $x=0$ to the point at $U=10^{-6}U_F$.
66041000	Shorten as 660410. LWC-TkB transistor with the full-length open-circuit remote body contact and the short-circuit point contact at the source ($x=\infty, y=0$). Subtracting flatband current. The thickness of drain current is from $x=0$ to $x=\infty$.
66041100	Shorten as 66041I. LWC-TkB transistor with the full-length open-circuit remote body contact and the short-circuit point contact at the source ($x=\infty, y=0$). Subtracting flatband current. The thickness of drain current is from $x=0$ to the point at $U=10^{-6}U_F$.
66040100	Shorten as 66040I. LWC-TkB transistor with the full-length open-circuit remote body contact and the short-circuit point contact at the source ($x=\infty, y=0$). Including flatband current. The thickness of drain current is from $x=0$ to the point at $U=10^{-6}U_F$.
6665010Y	LWC-TkB transistor with the short-circuit body contact from the source ($x=\infty, y=0$) to ($x=\infty, y=y_{65}$) and the open-circuit body contact from ($x=\infty, y=y_{65}$) to ($x_{65}, y=L$). $Y_{65}=y_{65}/L = 0, 0.2, 0.4, 0.6, 0.8, 1.0$ are used. Including flatband current. The thickness of drain current is from $x=0$ to the point at $U=10^{-6}U_F$.

2.3 Models labeled by eight digits

To facilitate our discussion, we have extended our six-digit name convention [1] for the many models to eight-digits JJVVFXYY in order to give an at-once-glance recognition of the parameters of each of the many models. The seven models analyzed in this paper are summarized in Table 1. The first two digits JJ represent the drain-current-equation type: JJ=96 is the four-component theory in [9,10], JJ=66 is the double integral formulation in [7]. The second two digits VV represent the gate-voltage-equation type: VV=65 is the 1965-Sah-Pao equation in [2]. VV=04 is the 2004-Sah-Jie self-consistent equation in [10]. The 5th digit, F, indicates avoidance of divergent flatband current: F=0 including flatband current, F=1 subtracting flatband current. The 6th digit, X, indicates avoidance of divergent drain-current via x-integration-range or basewell-body-thickness. X=0 for $x=0$ to $x=\infty$ where $U_\infty=0$; X=1 for $x=0$ to $x=X_1$ a far distance where $U=10^{-6}U_F$; X=I for $x=0$ to the intrinsic potential point $x=x(U=U_F)$ used in 1966-Pao-Sah [7]. The 7th and 8th digits YY denote the remote contact length and types for the gate-voltage equation. YY=00 is the short-circuit body contact at $(x=\infty, y=0)$. YY=09 is the short-circuit contact to the full body length from the source $(x=\infty, y=0)$ to the drain $(x=\infty, y=L)$. YY=15 is the short-circuit contact to the lower half of the body length from $(x=\infty, y=0)$ to $(x=\infty, y=L/2)$.

3. Constant P_{IM} transistors

The inversion n-channel MOS transistors in this report have these device and materials parameters: $P_{IM}=5 \times 10^{17} \text{ cm}^{-3}$, $X_{OX}=35 \text{ \AA}$, $W/L=1 \mu\text{m}/1 \mu\text{m}$, and $T=300.00 \text{ K}$ giving $n_i=1.33348 \times 10^{10} \text{ cm}^{-3}$. The work function difference of the Aluminum/SiO₂ metal-gate is $4.679-4.029=+0.650 \text{ eV}$. The two vertical lines in Figs. 1 and 2 are the subthreshold voltage $V_{GF-th-sub}$ labeled by U_F for the gate voltage that gives the surface potential at the source $U(x=0, y=0)=U_{S0}=U_F$, and the threshold voltage V_{GF-th} labeled $2U_F$ at $U_{S0}=2U_F$. They are convenient demarcation lines for the four operation ranges: the accumulation, $V_{GF} \leq 0$; the deep-subthreshold $0 \leq V_{GF} \leq V_{GF-th-sub}(U_F)$; subthreshold $V_{GF-th-sub}(U_F) \leq V_{GF} \leq V_{GF-th}(2U_F)$; inversion to strong inversion $V_{GF-th}(2U_F) \leq V_{GF}$. To ease subscripts, we use V_{GF-U_F} and V_{GF-2U_F} for the subthreshold and threshold voltages. The figures can be enlarged 64 times to see the small symbols.

Figure 1 shows the results of six transistors or models (660401, 660411, 660410, 666501, 666511). Since the differences are very small, the drain current is given only for two transistors: the reference transistor 660401 including the flatband current (solid line) and 660411 excluding the flatband current (dash line). The deviations (or errors) of the five transistors from the reference transistor are shown in symbols. All are at the same biases: source voltage $V_S=0$ and substrate or remote contact voltage $V_B=0$, drain-source voltage $V_{DS}=3.0 \text{ V}$ and gate voltage $V_{GF}=V_{GB}-V_{FB}$ from 0.0 V to 8.0 V .

The two drain currents, 660401 (solid line) and 660411 (dash line) are not distinguishable except near flatband

($V_{GF}=0$ to 0.2 V) where the error or deviation of 660411 without the flatband current (inverted triangle) seems to reach 100% at flatband $V_{GF}=0$ but is expected to be zero because the flatband current of the reference transistor 660401, $I_{D-660401}(V_{GF}=0)$, diverges due to the flatband current in the infinitely thick body, just like the leakage diffusion current in a reverse-biased base-floating bipolar-junction transistor.

The deviation (symbols) of the five models from the reference 660401 are all small in the inversion range, $V_{GF} > V_{GF-2U_S}=0.9 \text{ V}$, falling on the numeric noise floor, about 10^{-15} from the 15 significant digits limit of the double precision 32-bit Intel Fortran and IMSL subroutines. As expected, in the subthreshold and deep-subthreshold ranges, the deviations of the five models are different, although all rather small until near flatband.

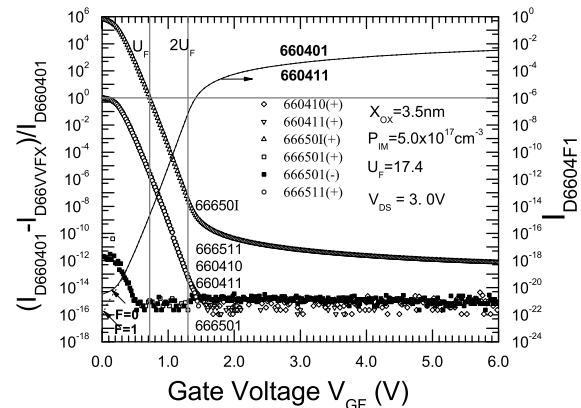


Figure 1 Drain current comparison of six models for the long-wide-channel-thick-base MOS transistor in the strong inversion range, the subthreshold or weak inversion range, and the deep subthreshold or near flatband range.

Transistor 66650I has the largest deviation (I=Intrinsic). It was used by 1966-Pao-Sah [7] which terminated the x-integration at a depth $x = x_1 = X_{INTRINSIC}$ where $U(x_1, y) = U_F$ because of IBM-7090's limited precision, but still the error drops exponentially from 100% as V_{GF} increases above the subthreshold-voltage V_{GF-U_F} . The next three largest deviations are $666511 > 660410 > 660411$, all nearly the same in the entire subthreshold and deep-subthreshold ranges approaching 100% at flatband. The smallest deviation is seen in model 666501 which uses the inconsistent remote boundary condition of 1965-Pao-Sah [7] but x-integration stops at $x=x_2$ or at $U(x_2, y) = 10^{-6}U_F$ to avoid the divergence.

Figures 2(a) and (b) show the effect from the geometry (length between source and drain) of the short-circuit body contact. The effect is expressed as the deviation of the drain current from that of the reference transistor 66650109 which has the short-circuit body contact of the 1965-Sah-Pao [2] at $x=\infty$ over the full length of the basewell-body from $Y=y/L=0$ to $Y=y_{65}/L=Y_{65}=1$. It is designated by the number 9 in 66650109 in order to avoid confusion with the $Y_{65}=0.1$ transistor. The body-contact model-transistors, 6665010Y, have the short-circuit body-contact over only a fraction of the body plane, i.e. from $(x=\infty, Y=y/L=0)$ to the

point ($x=\infty, Y=Y_{65}$), using the 1965-Sah-Pao x-equation or voltage-equation [2], which also allows body bias (not presented here to limit page-count). The remaining, from $Y=Y_{65}$ to $Y=1$ at $x=\infty$, has the open-circuit body-contact, using the 2004-Sah-Jie x- or voltage-equation [1,10].

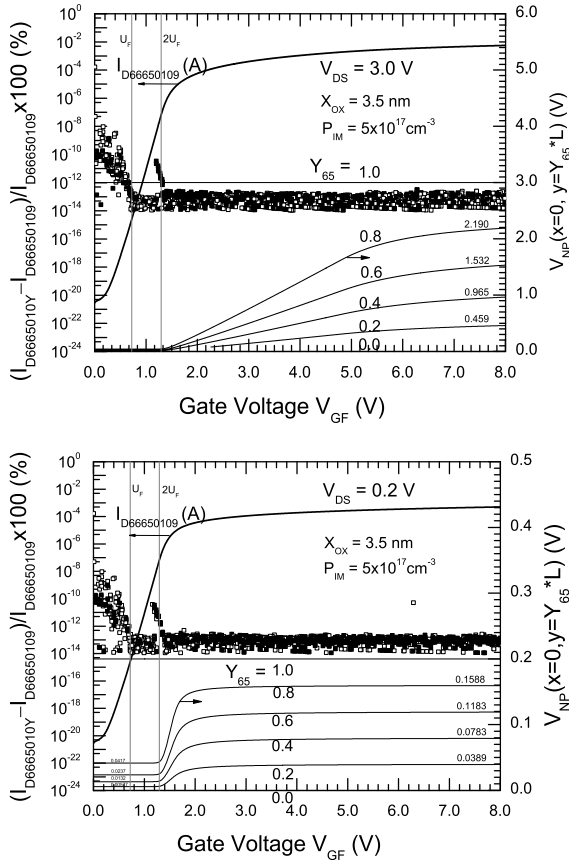


Figure 2 Effects of the length of the short-circuit basewell-body on drain current and its deviation, and on the interface hole-electron quasi-Fermi potential difference at the end point of the contact, $V_{NP}(x=0, y/L=Y_{65})$. (a) Drain current saturation range and (b) drain current linear range. Both in the strong inversion range.

Six transistors are computed ($Y_{65}=0.0, 0.2, 0.4, 0.6, 0.8, 1.0$). The percentage deviations of the drain current of the five transistors with the fractional-body-contact from that of the full-body-contact reference transistor $Y_{65}=1.0$ are computed in strong inversion at two drain voltages covering the drain current saturation range (a) $V_{DS}=3.0$ V and in the linear current range (b) $V_{DS}=0.2$ V. They are shown as symbols in Figs. 2(a) and 2(b). The deviations are small and fall on the numerical noise floor of the 32-bit Intel floating-point processor and Intel FORTRAN+IMSL subroutine $\sim 10^{-15}$. Figures 2(a) and 2(b) also give $V_{NP}(0, Y_{65})$ vs V_{GF} of the six transistors (six Y_{65} values) at the two V_{DS} . They all rise at the threshold voltage, $V_{GF}=V_{GF-2UF}$, when the channel becomes strongly inverted and conducting.

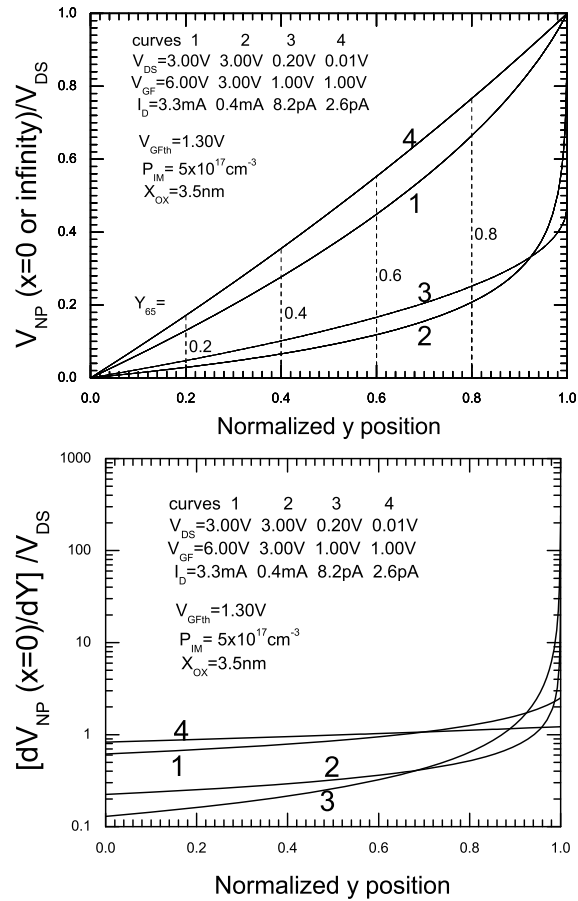


Figure 3(a) Longitudinal (channel length or y direction) variation of electron-hole quasi-Fermi-potential difference at the SiO_2/Si interface, $V_{NP}(x=0, y)$ solid lines, and at the body-basewell boundary, $V_{NP}(x=\infty, y)$ dashed lines. Fig 3(b) its gradient $(-\partial V_N / \partial y)$ at the SiO_2/Si interface $x=0$. Curve 1 strong-inversion linear drain-current range, Curve 2 strong-inversion drain-current saturation range, Curve 3 subthreshold drain-current saturation range, and Curve 4 subthreshold linear drain-current range.

The preceding fractional-body-contact model contains a discontinuity at the remote boundary line $Z=W$ located at ($x=\infty, y=y_{65}, z=W$) which separates the short-circuit contact from the open-circuit contact. This discontinuity is the abrupt jump from $V_{NP}(\infty, y \leq y_{65})=0$ to $V_{NP}(\infty, y_{65})$. At the SiO_2/Si interface, $x=0$, such an abrupt jump is not expected since the iteration solution would smooth the jump out and if existed a divergence in channel current density would result and observed in the graphs because $J_N(x=0, y_{65}) = q\mu_n N(0, y_{65})(-\partial V_N / \partial y)$. Numerical calculations are made and shown in Fig. 3(a) for $V_{NP}(x=\infty, y)$ and $V_{NP}(x=0, y)$, and in Fig.3(b), for $(\partial V_N / \partial y)$ at only $x=0$, since our model already tell us the existence of the jump of $V_{NP}(x=\infty, y_{65})$. The discontinuity of $V_{NP}(0, y_{65})$ is indeed smoothed. The four curves in Figs. 3(a) and 3(b) are for four bias points in the four ranges of distinct device-internal and device-terminal or -external current-voltage characteristics. They

are: the linear drain-current range (curves 1 and 4), the drain-current saturation range (curves 2 and 3), the strong inversion or drift-dominant current range (curves 1 and 2), and subthreshold or diffusion-dominant current ranges (curves 3 and 4). Their biases shown in the inset of Fig. 3(a) are related as follows to the threshold voltage where $V_{GF-2UF}=V_{GF-th}$ =values given here. Curves 1: $V_{DS}=3.00V < V_{GF}-V_{GFth}=4.70V$, $V_{GF}=6.00 > V_{GFth}=1.30V$, so it is in the strong-inversion linear drain-current range. Curves 2: $V_{DS}=3.00V > V_{GF}-V_{GFth}=1.70V$, $V_{GF}=3.00V > V_{GFth}=1.30V$, so it is in the strong-inversion drain-current saturation range. Curves 3: $V_{DS}=0.20V > 4kT/q=0.10V$, $V_{GF}=1.00 < V_{GFth}=1.30V$ so it is in the subthreshold drain-current saturation range. Curves 4: $V_{DS}=0.01V < 4kT/q$, $V_{GF}=1.00V < V_{GFth}=1.30V$, so it is in the subthreshold linear drain-current range.

4. Spatially Varying $P_{IM}(0,Y)$ Transistor

When the concentration of the dopant impurity in the basewell-body varies with position, such as the halo profile from impurity ion implantation, the y -independent remote potential assumed to derive the surface-potential gate-voltage equation (x -equation) is no longer valid. For example, in the short-circuit remote basewell-body contact model just described in section 3, the remote potential is a function of the $P_{IM}(y)$, thus a function of y -position.

A detailed description of the numerical algorithms using two iterative analytical drain current equations was given in [12]. The two iterative equations for models 66040100 and 66650109 are:

$$I_D = \frac{Z}{L} q D_n n_i L_{Di} \int_0^{U_S} dy \frac{dU_N}{dy} \exp(-U_N) \int_{10^{-6}U_F}^{U_S} \frac{\exp(+U)dU}{\text{sign}U_S \times F_X(U, U_N, U_P)} \quad (1)$$

$$\frac{\partial U_N}{\partial y} = I_D \left(Z q D_n n_i L_{Di} \int_{10^{-6}U_F}^{U_S} \frac{\exp(U - U_N)}{\text{sign}U_S \times F_X(U, U_N, U_P)} dU \right)^{-1} \quad (2)$$

As discussed in [12], there were convergence problems in the subthreshold range when the numerical algorithm was implemented using DEC 64-bit FORTRAN and the 32-bit IMSL subroutines on the 64-bit 433-MHz Alpha Station running OpenVMS 7.1. In the present investigation, we moved our DEC FORTRAN to an IBM-Lenovo T60 Thinkpad laptop computer with a 32-bit 1.83GHz Intel Core-Dual processor running the MicroSoft WindowsXP-PRO in order to run the Intel Visual Fortran and the Intel-IMSL subroutine. The convergence difficult seemed more severe, due to the 32-bit limitation. The algorithm can converge only in the strong inversion range. A second algorithm, using y as the variable instead of $U_N(y)$, to avoid the specific difficulty was developed but its testing was incomplete. Therefore, in this conference proceedings report due March 18, 2007, we shall report only one computation to demonstrate the effects of the remote contact types on the drain current of a long-wide-channel thick-base inversion channel nMOS transistor with $P_{IM}(y)$ in the p-basewell varying between the source and the drain.

Figure 4 shows the percentage difference of the drain current in the strong inversion range between 66650109 (the full length short-circuit remote basewell-body contact)

and 66040100 (the full length open-circuit remote basewell-body contact). The transistor in Fig.4 has a U shaped dopant impurity concentration profile described by

$$P_{IM}(y) = P_{IM0} + P_{IMS} \left\{ \exp \left\{ - \left[\frac{(Y-Y_S)}{\Delta_S} \right]^S \right\} \right\} + P_{IMD} \left\{ \exp \left\{ - \left[\frac{(1-Y-Y_D)}{\Delta_D} \right]^D \right\} \right\} \quad (4)$$

where $Y=y/L$, $P_{IM0}=0$, $P_{IMS}=P_{IMD}=3 \times 10^{17} \text{ cm}^{-3}$, $Y_S=Y_D=0$, $\Delta_S = \Delta_D = 0.374$, and $S=D=2$. Figure 4 shows that the percentage difference increases very quickly when the gate voltage decreases and approaches the threshold voltage. The computation by the PC stopped and no result was obtained in the subthreshold range where the difference increases exponentially. This does demonstrate the anticipation that the basewell-body contact type (and hence also geometry) should substantially affect the subthreshold and turn-off (or deep-subthreshold) current of the MOST.

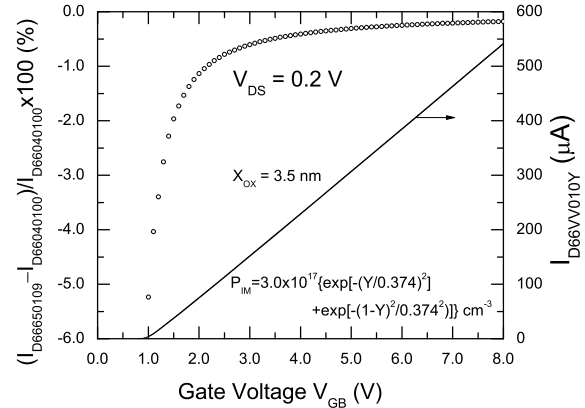


Figure 4: Comparison of drain current of two models: 66040100 full-length short-circuit basewell-body contact 66650109 full-length open-circuit basewell-body contact

5. Summary

The effects of the remote basewell-body contact type and contact geometry on the drain-current versus gate-voltage characteristics of long-wide-channel and thick-base MOS transistor are report in this paper. The effects are small in the inversion range and increasingly large in the subthreshold and deep-subthreshold flatband range, as anticipated also by device physics or analysis consideration, because the whole (infinitely) thick basewell or body would contribute increasingly the drain current as we approach flatband. The analysis provides an accurate estimate from analytical solution, which lead to the increasing influence as the basewell-body thickness is reduced, to the asymptotic or new geometries of double gate and SOI, both with thin basewell body.

Acknowledgments

The authors thank Drs. Gennady Gildenblatt, Colin McAndrew, Mitiko Miura-Mattausch, and Xing Zhou for their encouragement and suggestions. This investigation was supported by the CTSah Associates (CTSA) which was founded by the late Linda Su-Nan Chang Sah. The results presented in the figures were computed by Bin B. Jie during his leave at Florida from January 11 to March 10, 2007.

References

[1] Chih-Tang Sah and Bin B Jie, "A history of MOS Transistor Compact Modeling," Keynote. Proc.WCM-2005, Paper 1, pp.1-2; Full text, pp.347-390. May 10, 2005. Anaheim, CA, USA.

[2] Chih-Tang Sah and Henry C. Pao, "The effects of fixed bulk charge on the characteristics of metal-oxide-semiconductor transistors," IEEE Trans. ED-13(4), 393-405, April 1966. (1965-Sah-Pao)

[3] Narain Arora, *MOSFET Models for VLSI Circuit Simulation, Theory and Practice*, Springer-Verlag, Wien, New York, 1993, Chapter 6, pp.230-324. See the same pages in the reprint-volume of the ASSET Series of the World Scientific Publishing Company, Singapore, London and New Jersey, USA. January 2007.

[4] Chenming Hu, "From CMOS to Nanotechnology," Keynote at the 17th IEEE/SEMI Advanced Semiconductor Manufacturing Conference and Workshop (ASMC2006), May 22-24, 2006., Boston. Available from the Speaker. (www.semi.org/asmc)

[5] Josef Watts, Colin McAndrew, and Christian Enz, Carlos Galup-Montoro, Gennady Gildenblat, Chenming Hu, Ronald van Langevelde, Mitiko Miura-Mattausch, Rafael Rios, and Chih-Tang Sah, "Advanced compact models for MOSFETs," Invited, Proc. WCM-2005, Paper 2, pp.3-12. May 10, 2005.

[6] Carlos Galup-Montoro and Marcio Cherem Schneider, *MOSFET Modeling for Circuit Analysis and Design*, World Scientific Publishing Company, Singapore, New Jersey, 418pp, Chapter 12, January 2007.

[7] Henry. C. Pao and Chih-Tang Sah, "Effects of diffusion current on the characteristics of metal-oxide-semiconductor transistors," Solid-State Electronics, 9(10), 927-937, October 1966. (1966-Pao-Sah)

[8] Colin C. McAndrew and James J. Victory, "Accuracy of approximations in MOSFET charge models," IEEE Trans. ED-49(1), p. 72, January 2002. Weimen Wu, T-L Chen, G. Gildenblat, C. C. McAndrew, "Physics-based mathematical conditioning of the MOSFET surface potential equation," IEEE Trans. ED-51(7), 1196-1200, 2004. (2002-Gildenblat-McAndrew-Victory).

[8A] Notes added during proof.

We are indebted to Professor Gennady Gildenblat for the following two statements by email on Monday, March 19, 2007 14:46 from Tokyo where he was attending the ICMTS. He states:

1. In [8] we not only pointed (out) the problem but suggested a solution that turned out to be identical to the result that you have obtained subsequently using modified boundary conditions. This is worth pointing out to escape misunderstanding by people who are not totally familiar with the literature.

2. Apart from the mathematical conditioning, in [8] we have traced the problem to the position dependence of the minority (carrier) imref. This point of view is in fact confirmed by your work: new boundary conditions deal with the position dependence of the imref.

We (Jie and Sah) would like to add that the self-consistent and rigorously proven solution we obtained in [1] and used in [10] assumed strictly a position independent minority as well as majority carrier imrefs in order to give the analytical self-consistency and remove the imaginary flatband electric field. We also identified the physics underlying the constant imref assumption, which is, zero recombination both in the basewell-body-bulk region and also the back surface contact, such as the MOS without interface traps stated in these articles and also the present article, called the open-circuit body-basewell contact. We also demonstrated in this present article that the position dependence of the minority carrier imref that gave the not-selfconsistent 1965-Sah-Pao [2] boundary condition of infinite recombination velocity or short-circuit contact, gives very small drain current deviation, about $10^{-15}\%$ in the inversion range, rising exponentially to $10^{-11}\%$ with gate voltage from the threshold through subthreshold to flatband. This is the 40+year old self-inconsistent boundary condition, with the minority carriers missing, resolved by McAndrews-Victory-Gildenblat in references in [8].

[9] Chih-Tang Sah, "Space-Charge Theory of the MOS Transistor," Dec. 12, 1996 and March 31, 1997. Presented in: Bin B. Jie and Chih-Tang Sah, "Evaluation of a surface-potential-based bulk-charge model for MOS transistors," IEEE Trans. ED-52(8), pp 1787-1794, August 2005. (1996-Sah-Jie)

[10] Bin B. Jie and Chih-Tang Sah, "Accuracy of surface-potential-based long-wide-channel MOS transistor compact models," Invited, Proceedings on Compact Disk, WCM-2006, Paper 6, Vol. 3, pp. 622-630. May 9, 2006. (9604-four-component model)

[11] John R. Brews, "A charge-sheet model of the MOSFET," Solid-state Electronics 21(4), 345-355, April 1978. (1978-Brews)

[12] Bin B. Jie and Chih-Tang Sah, "Implementing Spatial Variation of Impurity Concentration in MOS transistor Modeling," Invited, Proceedings of 8th ICSICT-2006, pp. 1220-1226, Oct. 23-25, 2006.

[13] Chih-Tang Sah, *Fundamentals of Solid-State Electronics*, World Scientific Publishing Company 1991.